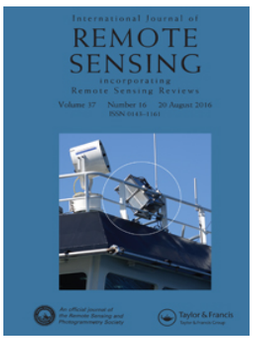

International Journal of Remote Sensing

ISSN: 0143-1161 (Print) 1366-5901 (Online) Journal homepage: https://www.tandfonline.com/loi/tres20

Analyzing the status of submerged aquatic vegetation using novel optical parameters

Luiz H. S. Rotta, Deepak R. Mishra, Enner H. Alcântara & Nilton N. Imai

To cite this article: Luiz H. S. Rotta, Deepak R. Mishra, Enner H. Alcântara & Nilton N. Imai (2016) Analyzing the status of submerged aquatic vegetation using novel optical parameters, International Journal of Remote Sensing, 37:16, 3786-3810, DOI: 10.1080/01431161.2016.1204027

To link to this article: https://doi.org/10.1080/01431161.2016.1204027

INTERNATIONAL JOURNAL OF REMOTE SENSING, 2016
VOL. 37, NO. 16, 3786–3810
http://dx.doi.org/10.1080/01431161.2016.1204027

Taylor & Francis
Taylor & Francis Group

Analyzing the status of submerged aquatic vegetation using novel optical parameters

Luiz H. S. Rotta[a], Deepak R. Mishra [b], Enner H. Alcântara [a] and Nilton N. Imai[a]

[a]Department of Cartography, São Paulo State University, Presidente Prudente, Brazil; [b]Center for Geospatial Research, Department of Geography, University of Georgia, Athens, GA, USA

ABSTRACT

The reservoirs constructed throughout Brazil for electrical power generation following its industrial and socioeconomic development now favour abundant aquatic macrophyte growth. Nova Avanhandava Reservoir is fully inhabited by submerged aquatic vegetation (SAV) that poses serious ecological and economic threats. The overall goal of this study was to assess the radiation availability in the water column in the Nova Avanhandava Reservoir and analyse its influence on SAV development and growth. In addition to the diffuse attenuation coefficient (K_d) and euphotic zone depth (Z_{EZ}), optical parameters such as percentage light through the water (PLW) were computed and analysed to achieve the objective. Nineteen sampling locations were considered for both spectroradiometer measurements and water sampling for analytical determination of total suspended solids (TSS) and chlorophyll-*a* concentration. Depth, SAV height, and precise position were also collected through hydro-acoustic measurements. The upstream region showed the highest TSS and K_d levels compared to the downstream. SAV heights were found to be lower upstream compared to downstream. The growth of tall SAV was favoured by low PLW, which grew taller to intercept required radiation. Locations with high transparency (lower K_d) also favoured the development of tall SAV compared to areas of high K_d. This may mean that low PLW values favour tall SAV growth if K_d is low enough not to hinder this. An inverse relationship between SAV height and attenuation of photosynthetic active radiation ($K_{d,PAR}$) was observed with a coefficient of determination of $R^2 = 0.56$ ($p < 0.001$), demonstrating that SAV height can be estimated using $K_{d,PAR}$ with significant accuracy.

ARTICLE HISTORY
Received 26 October 2015
Accepted 11 June 2016

1. Introduction

Nearly 90% of the area flooded by dams in Brazil is a direct consequence of the hydroelectric installations established in the last 40 years in the southwestern, west central, and southern regions (Araújo-Lima et al. 1995). Several dams constructed throughout Brazil for electric power generation following its industrial and socioeconomic development yielded many

CONTACT Deepak R. Mishra dmishra@uga.edu Center for Geospatial Research, Department of Geography, University of Georgia, 210 Field Street, Room 204, Athens, GA 30602, USA; Luiz H. S. Rotta luizhrotta@yahoo.com.br Department of Cartography, São Paulo State University, Presidente Prudente, SP, Brazil

artificial lake ecosystems (Esteves 2011). Reservoirs and natural lakes differ in significant ways, but there are many functional similarities between these ecosystems (Wetzel 2001). The processes and functions that are common to reservoirs and lakes include internal mixing, gas exchange across air–water interface, redox reactions, nutrient uptake, predator–prey interactions, and primary production. The main primary producers in reservoirs are the same as in rivers and lakes and primarily include phytoplankton, periphyton, and aquatic macrophytes (rooted, floating, emerged, and submerged) (Tundisi and Tundisi 2008). Macrophytes are vital in maintaining biodiversity (e.g. aquatic invertebrates, fish, and aquatic birds) in these freshwater systems because of their numerous important functions such as influencing nutrient cycling, maintaining water and sediment chemistry, proving food and shelter for various invertebrates and vertebrates, and changing the spatial structure of the waterscape by increasing habitat complexity (Thomaz et al. 2008). In addition, because submerged macrophytes occupy key interfaces in aquatic ecosystems they have major effects on productivity and biogeochemical cycles of the system (Carpenter and Lodge 1986). *Egeria densa* and *Egeria najas* are among the primary species of submerged macrophytes found in Brazilian reservoirs (Thomaz and Bini 1998; Cavenaghi et al. 2003; Marcondes, Mustafá, and Tanaka 2003; Bini and Thomaz 2005).

Several factors impact aquatic macrophyte primary productivity, such as temperature, radiation availability, stream velocity, water level variation, nutrient concentration, competition, and inorganic carbon (Caffrey, Hoyer, and Canfield 2007; Camargo, Pezzato, and Henry-Silva 2003; Biudes and Camargo 2008). However, radiation availability is the primary limiting factor for submerged aquatic macrophytes (Schwarz, Wintonb, and Hawes 2002; Havens 2003; Tavechio and Thomaz 2003; Thomaz 2006; Rodrigues and Thomaz 2010; Kirk 2011). In traversing the water column, the radiation changes primarily due to the concentration of materials in both solution and suspension such as chlorophyll-*a* (chl-*a*), total suspended solids (TSS), and coloured dissolved organic matter (CDOM) (Mishra et al. 2006; Esteves 2011; Mishra et al. 2013, 2014). Most of these materials in the water column absorb and scatter radiation and are referred to as optically active components (OACs). Studies on five Tietê River reservoirs in the state of São Paulo, Brazil showed that suspended solids have a major effect on light transmission through the water column and, thus, determine the development of submerged aquatic vegetation (SAV) (Cavenaghi et al. 2003).

Numerous studies have been conducted in an attempt to obtain better understanding of SAV behaviour in both coastal and estuarine waters, and freshwaters (Twilley et al. 1985; Kemp et al. 2004; Havens 2003). Many of these studies have concluded that the availability of photosynthetic active radiation (PAR) is the main limiting factor controlling SAV growth, and therefore use of the diffuse attenuation coefficient (K_d) of PAR ($K_{d,PAR}$) is required to assess the light availability for SAV (Gallegos 2001). Light penetration through the water column is controlled by OACs that are either dissolved or suspended in the water. Kemp et al. (2004) concluded that quantitative understanding of the mechanisms by which various OACs affect the transmission of light through the water column is important in order to estimate the potential availability of light for supporting SAV growth. The incident light is attenuated through the water column overlying submerged plants by OACs (chl-*a*, TSS, CDOM), by the epiphytic materials accumulated on SAV leaves, and by the water column itself. The transmission of incident light to SAV can be measured by two parameters: percentage light through the water (PLW) and percentage light at the leaf (PLL) (Kemp et al. 2004). PLW is the measure of the light transmitted through the water column to the depth of SAV growth, that is, depth

at the top of the macrophyte canopy, and PLL accounts for the additional light attenuation either by the epiphytic materials (attached algae) or settled materials (organic and inorganic solids) (Kemp et al. 2004). In other words, while PLW is a proxy for the light attenuated by the OACs in the water column, PLL is a proxy for ambient light that actually reaches the SAV leaves. These parameters have been conceptualized and used by the United States Environmental Protection Agency (U.S. EPA) for evaluating minimum light requirement for Chesapeake Bay SAV. However, to the best of our knowledge, these parameters have not been studied in lakes and reservoirs outside the US to analyse SAV growth. Although many laboratory-based studies have been conducted to evaluate the influence of PAR availability on the SAV in Brazilian reservoirs (Tavechio and Thomaz 2003; Rodrigues and Thomaz 2010), studies on SAV growth based on $K_{d,PAR}$, euphotic zone depth (Z_{EZ}), and optical parameters such as PLW and OACs are non-existent. Therefore, the overall goal of this study was to assess radiation availability in the water column in the Nova Avanhandava Reservoir and analyse its influence on SAV development and growth. The specific objectives included (i) computation and analysis of $K_{d,PAR}$ in the reservoir; (ii) estimation of PLW and Z_{EZ}; (iii) analysis of the relationship between SAV height and radiation availability and OACs.

Excessive growth of SAV is one of the main problems in Brazilian reservoirs. The uncontrolled growth of SAV can have many negative ecological and economic impacts on reservoir functions including water-based navigation, water quality and supply, hydropower, irrigation, fisheries, recreation, human and animal health, and land values (Jakubauskas et al. 2002; Rockwell 2003). According to Bini et al. (2005), reservoir construction often causes reduction in water velocity, water transparency, sediment stability, and water level control, and as a consequence creates suitable conditions for abundant growth of SAV such as *E. densa, E. najas* and *Ceratophyllum demersum* in subtropical and tropical reservoirs. Mostly in the rainy season, increased runoff to the reservoirs results in the fragmentation of SAV, and floating vegetation often obstructs water passing though the turbines of the hydroelectric plants causing significant economic damage (Marcondes, Mustafá, and Tanaka 2003). Therefore, the SAV delineation and growth requirement information generated through this research can help reservoir managers in taking appropriate actions to control excessive SAV growth and maintain reservoir functions such as leisure, fishing, navigation, and power generation. Overall, it is important to improve our knowledge about the spatiotemporal dynamics of SAV in reservoirs and freshwater lakes in order to develop rational and suitable control measures to assist in hydroelectric power generation and fulfill community needs.

2. Materials and method

2.1. *Study area*

This study was conducted at Bonito River in Nova Avanhandava Reservoir, which is a tributary of the Tietê River in the Brazilian state of São Paulo (Figure 1). The 1100 km-long Tietê River is fully contained within São Paulo (SSRH/CRHi 2011). Its source is on the Serra do Mar escarpments, 22 km inland, and its mouth is at the Paraná River where the São Paulo state borders Mato Grosso do Sul (SSRH/CRHi 2011).

The Nova Avanhandava Reservoir is in the 19th Water Resources Management Unit, Lower Tietê (Unidades de Gerenciamento de Recursos Hídricos 19– Baixo Tiête/UGRHI 19– BT), along with the Três Irmãos Reservoir (Table 1). The UGRHI

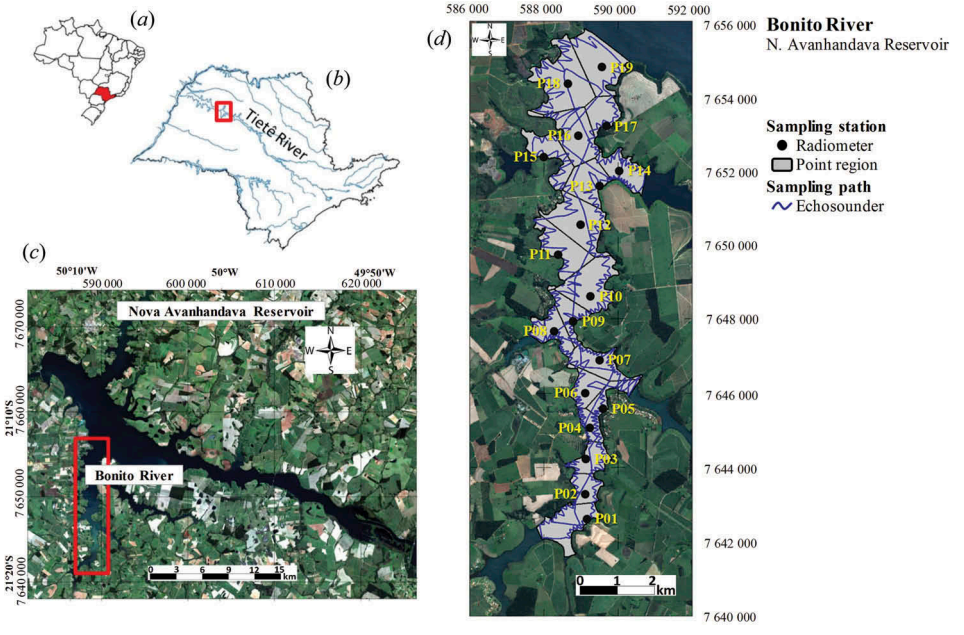

Figure 1. Location of the Nova Avanhandava reservoir in (*a*) Brazil and (*b*) São Paulo state. (*c*) A true colour satellite image acquired by Landsat OLI sensor shows the reservoir and the surrounding land use/land cover. The red rectangle indicates the actual research site (Bonito River). (*d*) Sampling locations (black dots), the hydro-acoustic data collection transects (blue line), and the regions used in analysis (grey polygon with black outline) are shown within the Bonito River; SPOT-6 bands 2, 1, 0 as RGB (9 July 2013; WGS-84; UTM 22S).

Table 1. Primary characteristics of the Nova Avanhandava Reservoir. Source: AES Tietê (2013).

Characteristic	Value
First year of operation	1982
Location	Tietê River, Rod. SP 461, km 44, Buritama– SP
Area (km^2)	210
Volume (m^3)	2.83×10^9
Dam length (m)	2038
Level difference (m)	29.7
Maximum useful height (m)	358
Minimum useful height (m)	356

19– BT has a 15,588 km^2 drainage area. The region's economy is primarily based on agriculture and cattle farming, but sugarcane cultivation has expanded recently and agro-industry is the most significant segments of local industry. Of the total area, 874 km^2 include vegetated areas (5.5% of the UGRHI area), and the primary formations are semi-deciduous forests and tree/shrub vegetation in floodplains (SSRH/CRHi 2011).

The Lower Tietê Basin geomorphology is characterized by a smooth relief with dissected plateaus that include rolling and gentle hills, as well as sedimentary landforms with alluvial plains and river terraces (CBH-BT/CETEC 1999). The Lower Tietê UGRHI is influenced by

continental tropical and Antarctic polar air masses. The rainfall pattern is typically tropical with a rainy season from October to April, a dry season from May to September, and annual precipitation that varies between 1000 and 1300 mm (CBH-BT/CETEC 1999). Winter is typically humid and mild with little rainfall. The minimum temperatures during the coldest month (July) range between 14 and 22°C. Summer is hot and humid with strong rains, and the temperatures oscillate between 24 and 30°C (CBH-BT/CETEC 1999).

Effluent discharged into the Tietê River upstream by Sao Paulo City causes high nutrients and suspended solids concentrations. However, reservoirs can help in the absorption of nutrients by organisms and decantation of suspended solids. Thus, Nova Avanhandava reservoir presents low nutrients concentration in the water and high transparency (Rodgher et al. 2005). This characteristic supports SAV development. A study conducted in 2001/2002 showed that the major macrophytes in Nova Avanhandava are *E. densa* and *E. najas* (submerged), *Typha angustifolia* and *Cyperus difformis* (emergent), and *Eichhornia crassipes* and *Eichhornia azurea* (floating) (Cavenaghi et al. 2003).

2.2. *Field data*

Nineteen sampling locations were considered for both spectroradiometric measurements and water sampling for analytical determination of TSS and chl-*a* concentrations (Figure 1(d)). Measurements were carried out between 28 and 30 June 2013. Based on the sampling locations, the river was split into 19 regions (grey polygon) represented by the Voronoi diagram to assess the relationship between water quality parameters and SAV behaviour. Those regions were drawn according the shortest distance among the sampling locations. During the field trip on 4 and 5 July 2013, data on SAV habitats were collected from each region using sonar equipment, which was mounted under a boat that followed the paths indicated in blue. Field data collected by echosounder BioSonics DT-X (http://www.biosonicsinc.com; Seattle, WA) included SAV height, water depth, and GPS position.

2.2.1. *OACs – TSS and chl-a*

At each sampling location, 7 l of water were collected from approximately 50 cm below the water surface. Bottles of 2 and 5 l were used for the analysis of TSS and chl-*a* concentration, respectively. During the fieldwork all the bottles were stored in a cooler to keep them at a cold temperature and in a dark environment until delivered to the laboratory for analysis. TSS extraction was performed following the method described in Clesceri, Greenberg, and Eaton (1998). The GF/F glass fibre filter discs were moistened and ignited in a muffle furnace at 550°C for 30 min, the discs were moistened again and dried in an oven at 103–105°C for 1 h, and finally, the filter discs were desiccated and weighed. Two litres of water were filtered using 47 mm diameter and 0.7 µm pore size. Filter sand filtrates were dried in an oven at 103–105°C for about 6 h and then combusted in a muffle furnace at 550°C for 30 min. The weights were measured after each step using a precision scale balance to derive fixed suspended solids (FSS), which represent the concentration of inorganic solids in suspension, and volatile suspended solids (VSS), which represent the concentration of organic solids in suspension; and TSS, which is the sum of the two above fractions. The same procedure was also followed to prepare replicates.

Chlorophyll-*a* concentrations were also derived for each sample using the method described in Golterman, Clymo, and Ohnstad (1978). Five litres of water were filtered

through GF/F glass fiber filters (47 mm diameter and 0.7 μm pore size), and chl-*a* was extracted from the filters using 90% acetone. The filters were macerated with acetone until smooth. The samples were inserted into a 10 ml graduated tube and centrifuged at 3500 rpm for 40 min. The absorbance at 663 and 750 nm was measured using a Femto 700 Plus spectrophotometer (http://www.femto.com.br/; São Paulo, SP; 195–1100 nm spectral range and 5 nm bandwidth). Absorbance were also measured at the same wavelengths after the addition of two drops of hydrochloric acid (0.1 N) to the samples. With these four readings (663 nm, 750 nm, 663 nm acidified, and 750 nm acidified), chl-*a* concentration was calculated for each sample and the replicates using Equation (1):

$$C_a = \frac{(U' - A')2.43 \times 10^6 \times V_a}{K_c \times V_f} \tag{1}$$

where

C_a: chl-*a* concentration;
$U' = U_{663} - U_{750}$: absorbance of non-acidified sample;
$A' = A_{663} - A_{750}$: absorbance of acidified sample;
V_a: centrifuged volume (10 ml);
K_c: absorption coefficient of chlorophyll-*a*;
V_f: filtered volume.

2.2.2. *Hyperspectral downwelling irradiance*

Hyperspectral downwelling irradiance (E_d) data collection is essential in estimating water column attenuation and radiation availability at the top of the SAV canopy (Mishra et al. 2005). E_d data were collected using the TriOS/RAMSES (ACC-VIS) optical sensor (http://www.trios.de; Rastede, Germany). The hyperspectral UV/VIS irradiance sensor has 190 channels from 320 to 950 nm, and a resolution of 3.3 nm with spectral accuracy of 0.3 nm. Hyperspectral E_d data were collected above the water surface, $E_{d,0+}$ (Figure 2(a)), just below the water surface $E_{d,0-}$ (Figure 2(b)), and at various depth Z intervals $E_{d,Z}$ (Figure 2(c)) in the water column at all 19 sampling locations. A depth interval of 0.5 m was used for

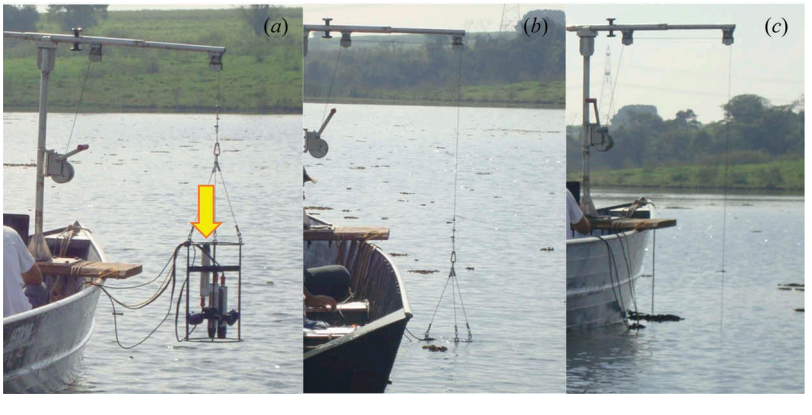

Figure 2. TriOS optical sensor deployment for E_d measurements (*a*) above water, (*b*) just below water surface, and (*c*) other depths.

sampling locations with SAV, and the last $E_{d,Z}$ reading was acquired about 1 m above the SAV canopy to prevent resuspension of particles adhered to the plant, which could have influenced the E_d measurements. A depth interval of 1.0 m was used for locations deeper than 10 m up to about 1% of $E_{d,0-}$.

2.2.3. *Echosounder data*

Water depth, SAV height, and precise position data were also collected through hydroacoustic measurements in order to assess the influence of vertical attenuation of E_d and OACs on SAV growth. Depth and SAV height data were collected between 3 and 5 October 2013 using the scientific digital sonar BioSonics DT-X Echosounder. Acoustic data recorded in numerous transects are represented by blue lines in Figure 1(d). The DTX Echosounder included a surface unit with a dedicated processor for operation, which generated the electrical signal and controlled the transducer. The transducer was connected to the surface unit by a cable and converted the electrical signal from the surface unit into an acoustic pulse and the pulse's echo into electric signal (Biosonics 2004a). An external communication device (notebook) connected via an ethernet interface was used to load the system operating parameters as well as display and store the data received from the echosounder. A GPS was connected to the surface unit and provided positional information for the acoustic data (Figure 3).

The echosounder transducer was vertically positioned at 0.5 m depth on the side of the boat, and the GPS antenna was positioned at the opposite end on the same pole. The data collected using the echosounder were visualized in real time via the notebook and stored in separate files for each transect. The system was controlled using the visual acquisition software, Biosonics, which displays an echogram that describes the submerged relief depth and the presence or absence of submerged aquatic macrophytes. The sensor emits 10 acoustic pulses every 2 s. After processing through EcoSAVsoftware, Biosonics, each set of 10 pulses yields a line in an ASCII file that contains the day, time of

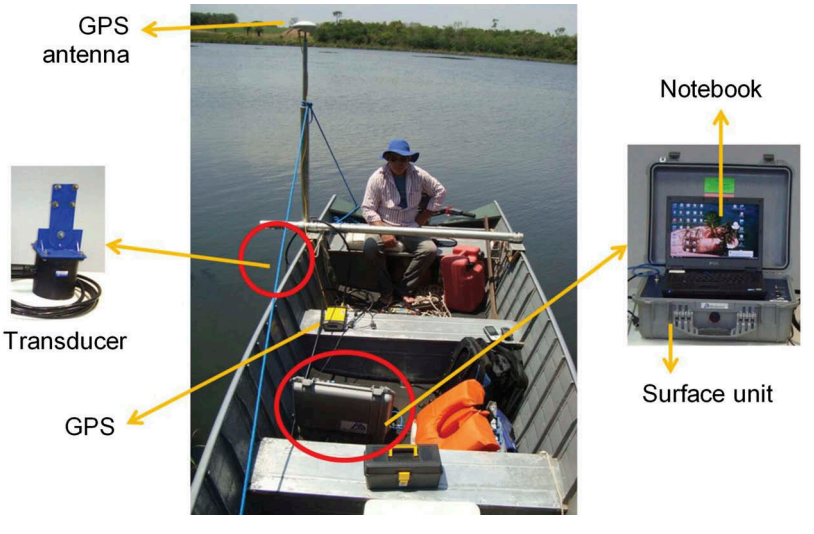

Figure 3. Components of the DT-X echosounder deployed to acquire depth and SAV height data along numerous transects.

day, position (lat., long.), depth (m), coverage (%), and mean height for the SAV (Biosonics 2008). Rotta et al. (2012) previously used this equipment and software for SAV mapping.

The echosounder data were collected in transects considering the targets with SAV (shallow water) and without SAV (deep water). This survey was conducted pursuing a spatial distribution and number of samples significant for the entire study area. More than 15,000 points were collected and divided into 19 regions. Descriptive statistics (min., max., range, average, and standard deviation) were computed for these data for each region, as shown in Table 2. The echosounder was calibrated as per the Biosonics recommendations (Biosonics 2004b) using a standard target sphere of known target strength (TS). The standard target is optimized in size, material, material purity, and dimensional tolerances to provide exceptional TS accuracy and stability.

In this study, the SAV height was measured with an echosounder using hydro-acoustic methods commonly used in previous studies. For example, Sabol et al. (2002) evaluated a Biosonics digital echosounder for detection of SAV using EcoSAV software. Divers measured the distances between the transducer face, top of the SAV canopy, and the bottom. Ground truth exhibited close agreement between true SAV height and the hydro-acoustic estimates ($R^2 = 0.78$). EcoSAV also was used by Chamberlain et al. (2009), who found similar agreement between ground truth and hydro-acoustic datasets. They also showed that the spatial differences in SAV coverage and height were accurately detected by the hydro-acoustic method.

2.3. *Data analysis*

2.3.1. *Data normalization*

Most uncertainties in measured K_d profiles result from changes in cloud cover that can cause variations in incident surface irradiance, E_s. According to Mueller (2003), frequent changes in cloud cover lead directly to variability of the in-water light field and must be corrected to obtain accurate estimations of optical properties from irradiance or radiance. Therefore, it is strongly recommended that all scans be normalized to a specific scan. The normalization factor, $N_{F,Z}$, for each scan at depth Z can be calculated as:

$$N_{F,Z} = \frac{E_{s,\,t(0-)}}{E_{s,\,t(Z)}} \tag{2}$$

where $E_{s,t(0-)}$ is the downwelling irradiance measured during the first scan at time $t(0–)$ on the boat, and $E_{s,t(Z)}$ is the downwelling irradiance measured at time $t(Z)$ on the boat. Figure 4(a) shows the radiometers that measured the downwelling irradiance on the boat (E_s), which was used to calculate $N_{F,Z}$ and the downwelling irradiance at water depth $Z(E_{d,Z})$ used for the computation of K_d.

A normalization factor greater than 1 indicates lower irradiance, such as cloud shadows, and values less than 1 indicate brighter conditions (Mishra et al. 2005). To normalize the spectral downwelling irradiance and eliminate the noise due to changes in illumination, Equation (3) was used:

$$E'_{d,Z} = E_{d,z}\, N_{F,Z} \tag{3}$$

Table 2. Descriptive statistics of SAV height for all sampling locations.

Sampling location	*n*	Average (m)	SD (m)	Min (m)	Q1 (m)	Median (m)	Q3 (m)	Max (m)
P01	825	0.48	0.22	0.11	0.30	0.49	0.64	1.58
P02	448	0.47	0.24	0.12	0.26	0.49	0.65	2.18
P03	561	0.51	0.24	0.13	0.30	0.52	0.66	1.73
P04	613	0.47	0.26	0.13	0.24	0.41	0.70	1.20
P05	616	0.68	0.28	0.14	0.46	0.73	0.88	1.45
P06	620	0.81	0.37	0.11	0.53	0.84	1.03	1.87
P07	956	0.77	0.32	0.11	0.53	0.77	0.97	1.77
P08	919	0.76	0.35	0.13	0.48	0.80	1.01	1.96
P09	734	0.68	0.26	0.12	0.50	0.69	0.86	1.78
P10	1315	0.71	0.32	0.09	0.51	0.73	0.92	3.20
P11	857	0.76	0.34	0.15	0.54	0.74	0.98	2.44
P12	1125	0.80	0.29	0.09	0.62	0.80	1.00	2.27
P13	696	0.78	0.36	0.14	0.48	0.86	1.00	2.75
P14	1025	0.85	0.44	0.12	0.54	0.89	1.07	2.96
P15	745	0.88	0.36	0.09	0.67	0.93	1.09	2.82
P16	902	0.96	0.35	0.18	0.76	1.02	1.18	2.58
P17	389	1.07	0.65	0.20	0.60	0.98	1.30	3.81
P18	1275	0.98	0.45	0.17	0.72	0.95	1.18	4.05
P19	754	1.00	0.43	0.09	0.73	1.03	1.25	4.55

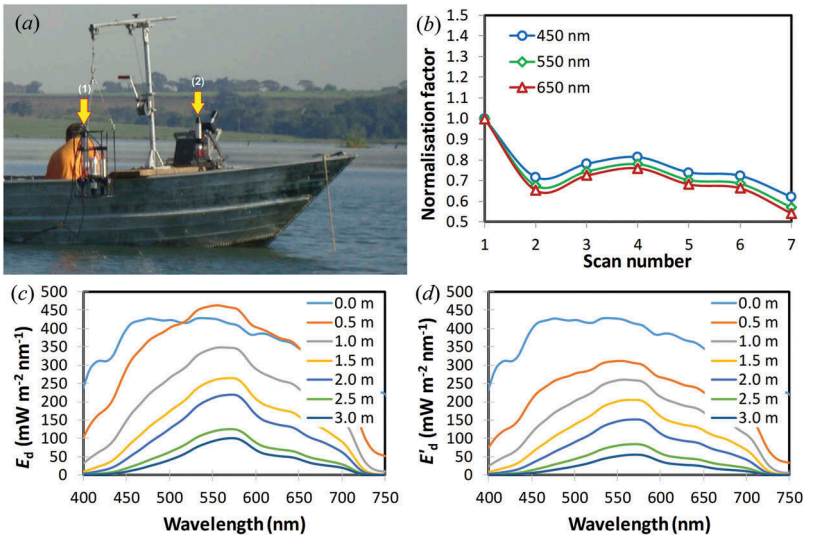

Figure 4. (*a*) Downwelling irradiance (E_d) measured at different depths (1) and downwelling irradiance (E_s) measured on the boat (2). (*b*) Normalization factor for each scan at P13 showing the variations in illumination conditions. Downwelling irradiance (*c*) before and (*d*) after normalization at P13.

The wavelengths 450 nm (Blue), 550 nm (Green), and 650 nm (Red) were selected to demonstrate how the sky conditions changed during the radiometric measurements (Figure 4(b)). The difference between downwelling irradiance before and after normalization for point P13 is shown as an example in Figure 4(c) and (d), respectively. Scan 1 and Scan 2 before normalization showed similar irradiance values which were erroneous, because the scans were acquired at different depths, that is, the depth at Scan 1 and Scan 2 was 0.0 m and 0.5 m, respectively (Figure 4(c)). The change in illumination conditions between the scans is evident in Figure 4(b), and therefore those variations were compensated by the normalization procedure given in Equation (3). The value of K_d was calculated for each sampling location after the normalization procedure.

2.3.2. K_d and Z_{EZ}

K_d, defined as the exponential decrease in ambient irradiance as a function of depth (Kirk 2011), is the parameter that controls the propagation of light through water. Characterizing the water column K_d is important because this can quantify the presence of light at different depths and determine the depth of the euphotic zone, which in turn controls the presence or absence of SAV (Mishra et al. 2005, 2007). K_d is derived using field-measured $E_{d,Z}$ as (Mobley 1994):

$$E_{d,z} = E_{d,0-}e^{-K_d Z} \tag{4}$$

where $E_{d,0-}$ is the downwelling irradiance just below the water surface and $E_{d,Z}$ is the downwelling irradiance at water depth Z.

All photosynthetic pigments such as chlorophyll and carotenoids absorb light energy from the underwater light field in the visible spectrum from 400 to 700 nm, known as

photosynthetically active radiation (PAR) (Kirk 2011). The PAR downwelling irradiance at water depth Z ($E_{d,Z,PAR}$) can be estimated by integrating $E_{d,Z}$ between 400 and 700 nm. Based on Equation (4), $K_{d,PAR}$ can be derived as:

$$E_{d,Z,PAR} = E_{d,0-,PAR}e^{-K_{d,PAR}Z} \tag{5}$$

where $E_{d,0-,PAR}$ is the PAR downwelling irradiance just below the water surface, $K_{d,PAR}$ is the downwelling diffuse attenuation coefficient of PAR light in the water column, and Z is the measured depth.

The most reliable estimates of light requirement by SAV can be determined by comparing *in situ* depth distribution of SAV to $K_{d,PAR}$ (Gallegos 2001). In addition, Z_{EZ} (euphotic zone depth) can be calculated using the PAR readings. The illuminated portion of the water column, the euphotic zone, can vary from a few centimetres to tens of metres. The euphotic zone is the region in a water body with sufficient PAR to sustain photosynthesis. Quantitatively, Z_{EZ} is defined as the depth at which the downwelling irradiance $E_{d,Z,PAR}$ falls to 1% of that just below the surface $E_{d,0-,PAR}$ (Kirk 2011), as indicated in Equation (6):

$$E_{d,Z,PAR} = 0.01E_{d,0-,PAR} \tag{6}$$

Combining Equations (5) and (6) yields the following:

$$0.01E_{d,0-,PAR} = E_{d,0-,PAR}e^{-K_{d,PAR}Z_{EZ}} \tag{7}$$

Solving Equation (7) yields:

$$\ln(0.01) = \ln e^{-K_{d,PAR}Z_{EZ}} \tag{8}$$

or

$$K_{d,PAR}Z_{EZ} = 4.6 \tag{9}$$

The $K_{d,PAR}$ and Z_{EZ} values were interpolated by inverse distance weighting (IDW) methods for the entire reservoir. In IDW, the interpolated points were calculated by weighted average of inverse distance (Isaaks and Srivastava 1989).

2.3.3. *Relationship between SAV height and radiation availability*

The hyperspectral E_d data measured at different depths were used to compute wavelength-specific K_d, $K_{d,PAR}$, and Z_{EZ} at each sampling location. The SAV heights and depths were determined using echosounder measurements. Boxplots with SAV height data at each depth were generated. Linear regressions between SAV height (average and maximum) and $K_{d,PAR}$ were fitted to determine the influence of radiation attenuation on the SAV development. In addition, PLW, which acts as proxy for radiation availability for SAV habitats, was computed. PLW was calculated as an exponential relationship to the depth of SAV growth (Z_{SAV}) and attenuation coefficient (K_d) (Equation (10)):

$$PLW = 100\ e^{-K_{d,PAR}Z_{SAV}} \tag{10}$$

Finally, based on the data collected using the echosounder, a dispersion plot was generated for SAV height as a function of depth for each region. Using that information,

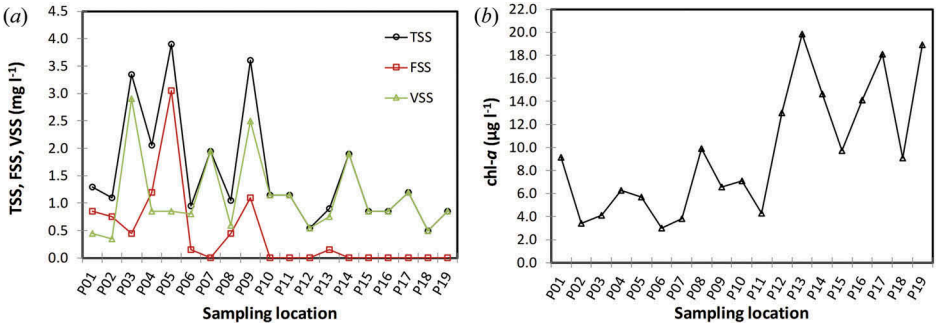

Figure 5. TSS, FSS, VSS, and chl-*a* concentration at each sampling location.

the influence of PAR availability by Z_{EZ} on SAV occurrence and development was analysed.

3. Results and discussion

3.1. *OACs – TSS and chl-a*

The TSS and chl-*a* concentrations were measured at 19 sampling locations and the values are shown in Figure 5. The range variability of TSS, FSS, and VSS was 3.4, 3.0, and 2.5 mg l^{-1}, respectively. The range variability of chl-*a* was 17 µg l^{-1}. As expected, the sampling located at the narrower portion of the reservoir showed the highest TSS level compared to the sampling at the wider end, mainly because of the speed of water flow. The VSS (organic fraction) spatial behaviour was similar to TSS. FSS (inorganic fraction) had significant values up to P09, and from points P10 to P19 values became close to zero. At downstream (close to P19) the water flow speed is typically lower because of the higher depth and width forcing FSS to be decanted. Further downstream, all suspended solids concentration (TSS, VSS, and FSS) showed reduced values; therefore, radiation attenuation was weaker. With increased radiation availability, phytoplankton (chl-*a*) development was favoured in those regions.

3.2. *K_d and Z_{EZ}*

E_d values were integrated over the wavelength range between 400 and 700 nm for each reading (depth) to obtain $E_{d,PAR}$. $E_{d,PAR}$ exhibited the exponential decay of $E_d$as described by Lambert–Beer's Law (Figure 6). Based on Equation (5), the slope value between $E_{d,PAR}$ and depth was assumed to be $K_{d,PAR}$. $K_{d,PAR}$ values for each point were used in the derivation of Z_{EZ} (Equation (9)). Figure 9(a) shows the $K_{d,PAR}$ and the Z_{EZ} values of each point in our study area. From the 19 values of $K_{d,PAR}$ and Z_{EZ}, 14 were used in the IDW interpolation (Figure 7) and five points were selected randomly to calculate the RMSE in order to validate the IDW results. The RMSE for K_d and Z_{EZ} was 9.93 and 8.29%, respectively.

Higher $K_{d,PAR}$ values were noted in the upstream areas, particularly around sampling locations 3, 4, and 5 of the river, which corresponded to lower Z_{EZ}; this means that at

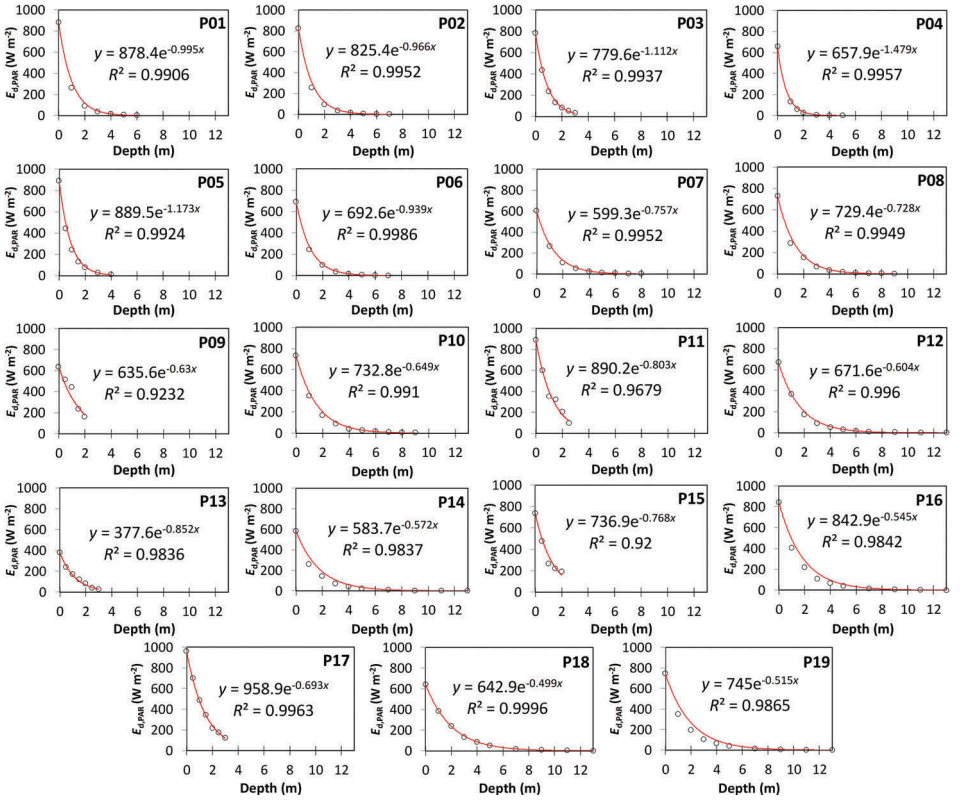

Figure 6. Vertical attenuation of $E_{d,PAR}$as a function of depth at each sampling location.

those locations the PAR barely penetrated through the water column. These upstream areas, which are relatively shallow compared to those downstream, often experience resuspension of bottom sediments induced by strong winds and water flow (Wetzel 2001; Cho 2007). However, an anthropogenic factor could be responsible for the higher TSS values upstream – the presence of a sand mining company between P03 and P04 (Figure 8). Sand extraction from the bottom of the river could be accelerating the sediment resuspension that increases K_d values at nearby locations.

In downstream areas, that is, those close to the Tietê River, higher Z_{EZ} values were observed. In those areas (P09 for example), slow water flow due to the dam and higher depths favoured the deposition of suspended solids on the bottom, which resulted in lower $K_{d,PAR}$. In addition to $K_{d,PAR}$, spectral K_d was also calculated for each point based on Equation (4) (Figure 9(b)). Spectral K_d showed a similar pattern to $K_{d,PAR}$. Upstream regions between P01 and P09 showed high values compared to downstream regions (P10–P19). That difference was greater mainly in the blue and green spectral range, where the effect of OACs was maximum compared to the red region where absorption by water itself plays a dominant role. $K_{d,PAR}$ also showed a positive correlation with TSS and negative correlation with chl-*a* concentration. Downstream regions with lower TSS and lower K_d have greater radiation availability through the water column, which favours phytoplankton growth and associated high chl-*a*.

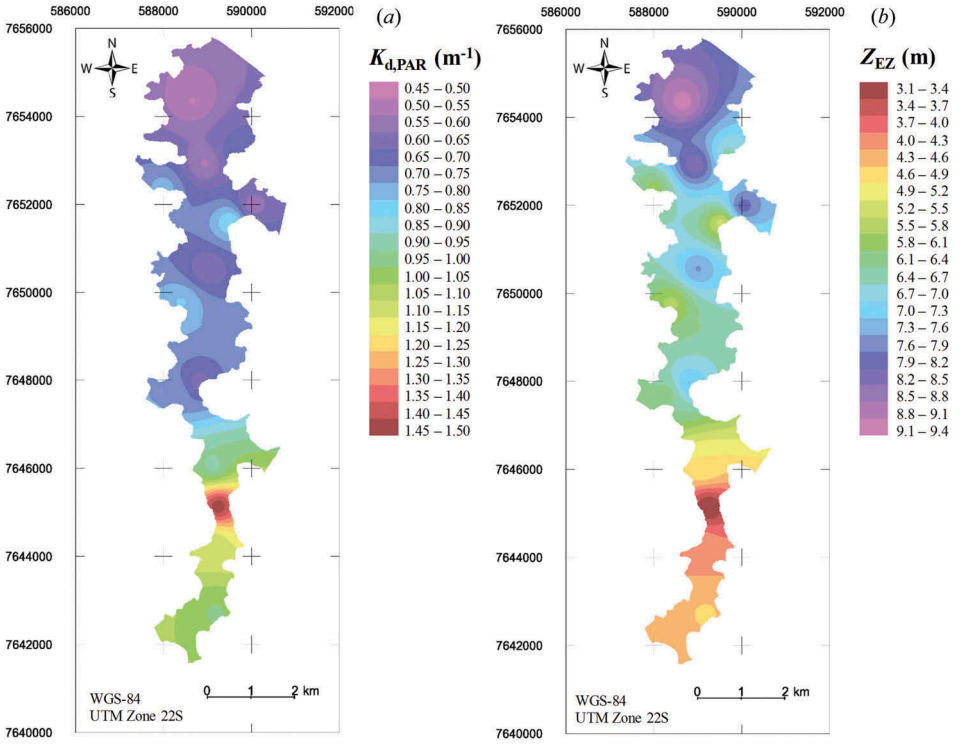

Figure 7. $K_{d,PAR}$ and Z_{EZ} of Bonito River using inverse distance weighting (IDW) interpolation.

Relationships between $K_{d,PAR}$ and TSS (Figure 9(c)) and chl-*a*(Figure 9(d)) were analysed at each sampling location. A positive relationship between TSS and $K_{d,PAR}$ (p = 0.05) was observed, which indicated that an increase in TSS reduced radiation availability in the water column and enhanced the K_d value. Since SAV development is directly influenced by radiation availability, regions with lower TSS (near to P19, downstream) favoured SAV growth. With increased radiation availability, phytoplankton (chl-*a*) development was favoured which produced an inverse relationship between $K_{d,PAR}$ and chl-*a* (p = 0.04).

3.3. *SAV height and radiation availability*

Table 2 shows the descriptive statistics of SAV height for each point region denoted by a grey polygon in Figure 1. The regions surrounding the upstream points (P01–P04) had lower average SAV height, with values up to 0.6 m. In the middle region of the river (P05–P15), average SAV height was found to be between 0.6 and 0.9 m. In the downstream region (P16–P19), the average SAV height was over 0.9 m. Interestingly, the minimum SAV height recorded was similar for all point regions, that is, the location of the point in the river did not influence the minimum SAV height.

Boxplots for SAV height variability relative to depth at each point region are shown in Figure 10. In general, SAV height values were lower around P01 (upstream) compared to areas near P19 (downstream). The range of SAV height between P01 and P19 was 3 m,

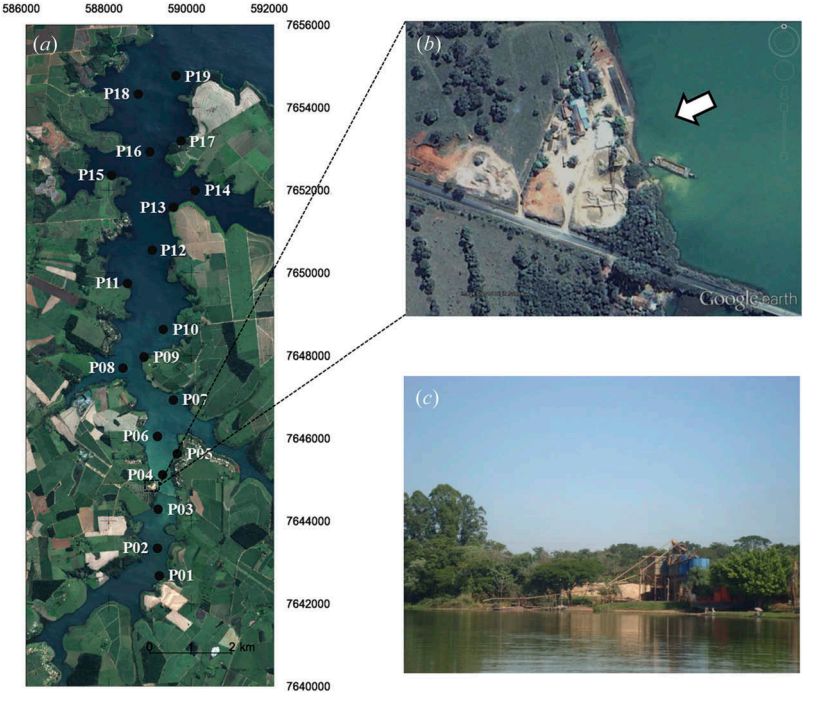

Figure 8. Bonito River in Nova Avanhandava reservoir with the sample points and the rectangle representing the location of the sand mining company. Data source: SPOT-6 image; 9 July 2013; WGS-84; UTM Zone 22S. Zoomed-in areas (*b*,*c*) showing the detailed location using Google Earth (accessed 10 May 2013).

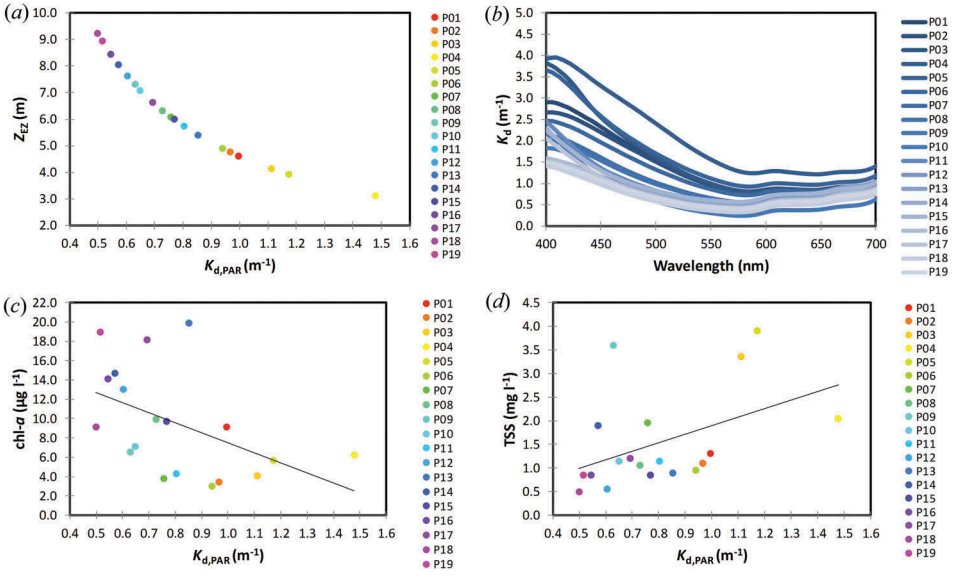

Figure 9. Relationship between $K_{d,PAR}$ and Z_{EZ} (*a*). Hyperspectral $K_d$at each sampling location (*b*). $K_{d,PAR}$ versus chl-*a* (*c*) and $K_{d,PAR}$ versus TSS (*d*).

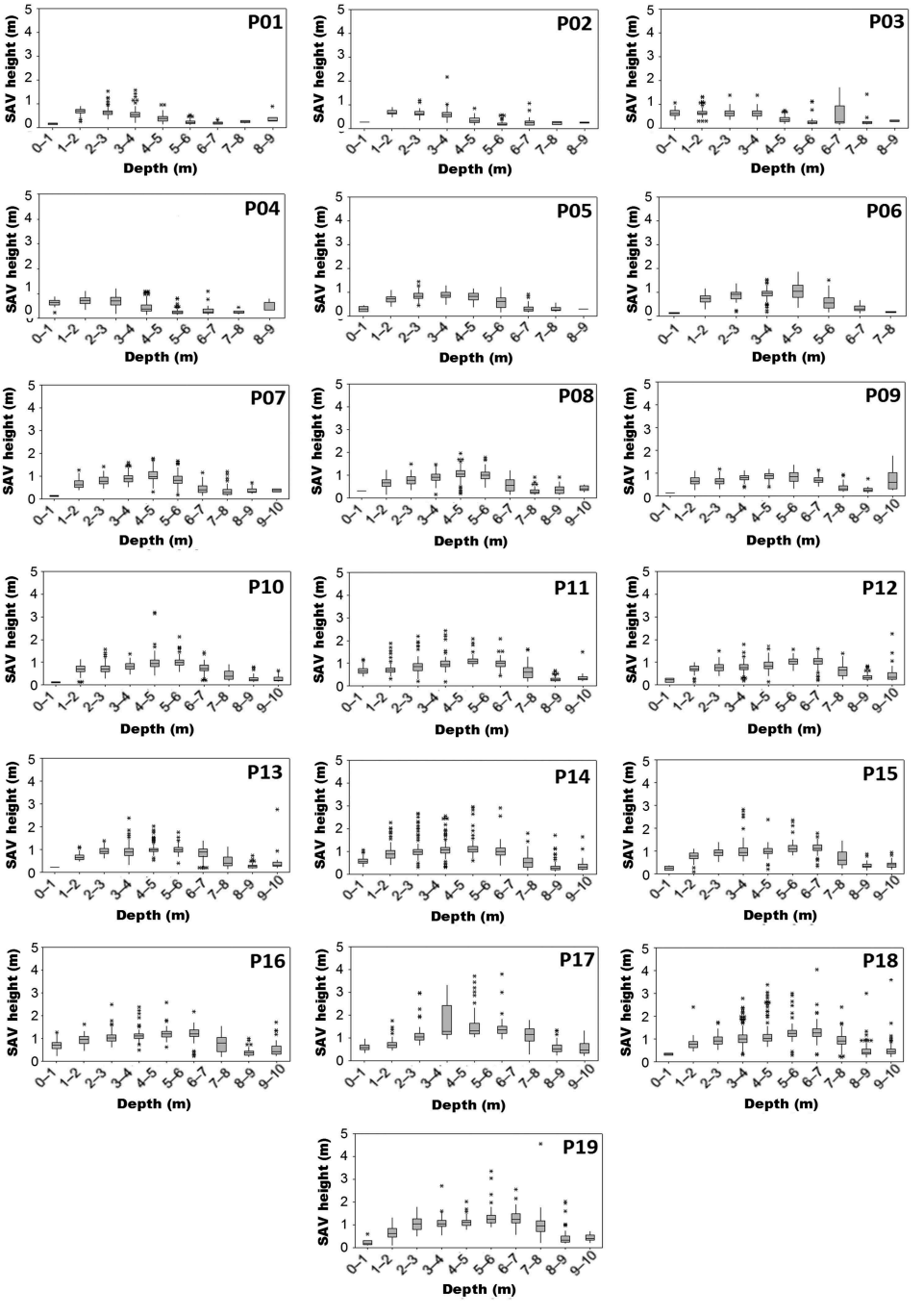

Figure 10. Boxplots for SAV height relative to depth at each sampling location.

that is, 1.5 m for P01 and 4.5 m for P19. The maximum depth of SAV development was clearly influenced by K_d, and SAV occurrence was observed at depths up to 10 m only in the downstream regions, that is, regions with the lowest $K_{d,PAR}$ values (P07–P19).

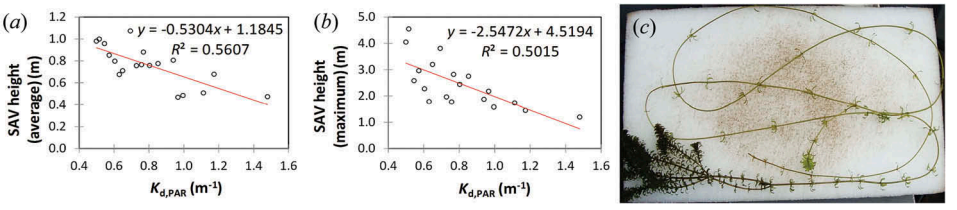

Figure 11. Relationship between (*a*) average SAV height and (*b*) maximum SAV height and $K_{d,PAR}$; (*c*) 3 m-long *Egeria sp*. acquired from the Nova Avanhandava Reservoir (SP, Brazil) during fieldwork.

Therefore, the average and maximum SAV height, height variability, and depth of occurrence of SAV were primarily influenced by K_d. Figure 11((a,b) shows the relationship between SAV height (average and maximum) and $K_{d,PAR}$ for each point region. The coefficient of determination (R^2) between average SAV height and $K_{d,PAR}$ was 0.56 (p = 0.0002) and between maximum SAV height and $K_{d,PAR}$ was 0.5 (p = 0.0007).

As expected, an inverse relationship between SAV height (average and maximum) and $K_{d,PAR}$ was observed. An increase in the attenuation of radiation in the water column resulted in a decrease in the likelihood of SAV development. The linear models demonstrated that SAV height can be estimated by $K_{d,PAR}$ in the study area with significant accuracy. Figure 12 shows the relationship between SAV height and SAV biophysical parameters such as PLW.

Overall, many PLW readings were 0 or close to 0 for low-SAV height locations, mainly due to interference from bottom reflectance. These extremely low values significantly interfered with and destroyed the relationship between PLW and SAV height. PLW peaked when SAV height was between 0.5 and 1.0 m, and a general exponential decay was observed as SAV height increased, primarily due to increased absorption by the top canopy and higher attenuation through leaves.

At sampling locations between P01 and P06 (upstream), where K_d values were close to or more than 1.0 m^{-1}, that is, lower water transparency than in downstream, SAV height did not have a well-defined relationship with PLW. However, an increase in SAV height was noted up to around 0.75 m with increase in PLW; after that, SAV height tended to decrease again. At sampling locations where K_d values were lower than upstream (P07– P19), an inverse relationship was observed between SAV height and PLW. This relationship is not strong, but it was observable that behaviour. At those stations, SAV height increased as PLW decreased. This may be due to the fact that SAV did not grow upward to receive as much PAR as possible in areas where PLW or PAR availability was higher. On the other hand, when PLW decreased SAV grew taller to receive the light required for its survival. However, it is important to know that growing tall does not necessarily mean higher biomass compared to shorter plants. At points between P14 and P19, there were locations where SAV height was greater than 2 m, particularly in regions with lower PLW. These points have the lowest K_d values, which indicated that the maximum height of SAV could be dependent on a combination of two parameters, PLW and K_d.

It should be noted that not all PLW is available to the SAV, because the light is attenuated either by epiphytic or settled materials. Percentage light at the leaf (PLL) is a proxy for ambient light that actually reaches the plant leaves. For example, Kemp,

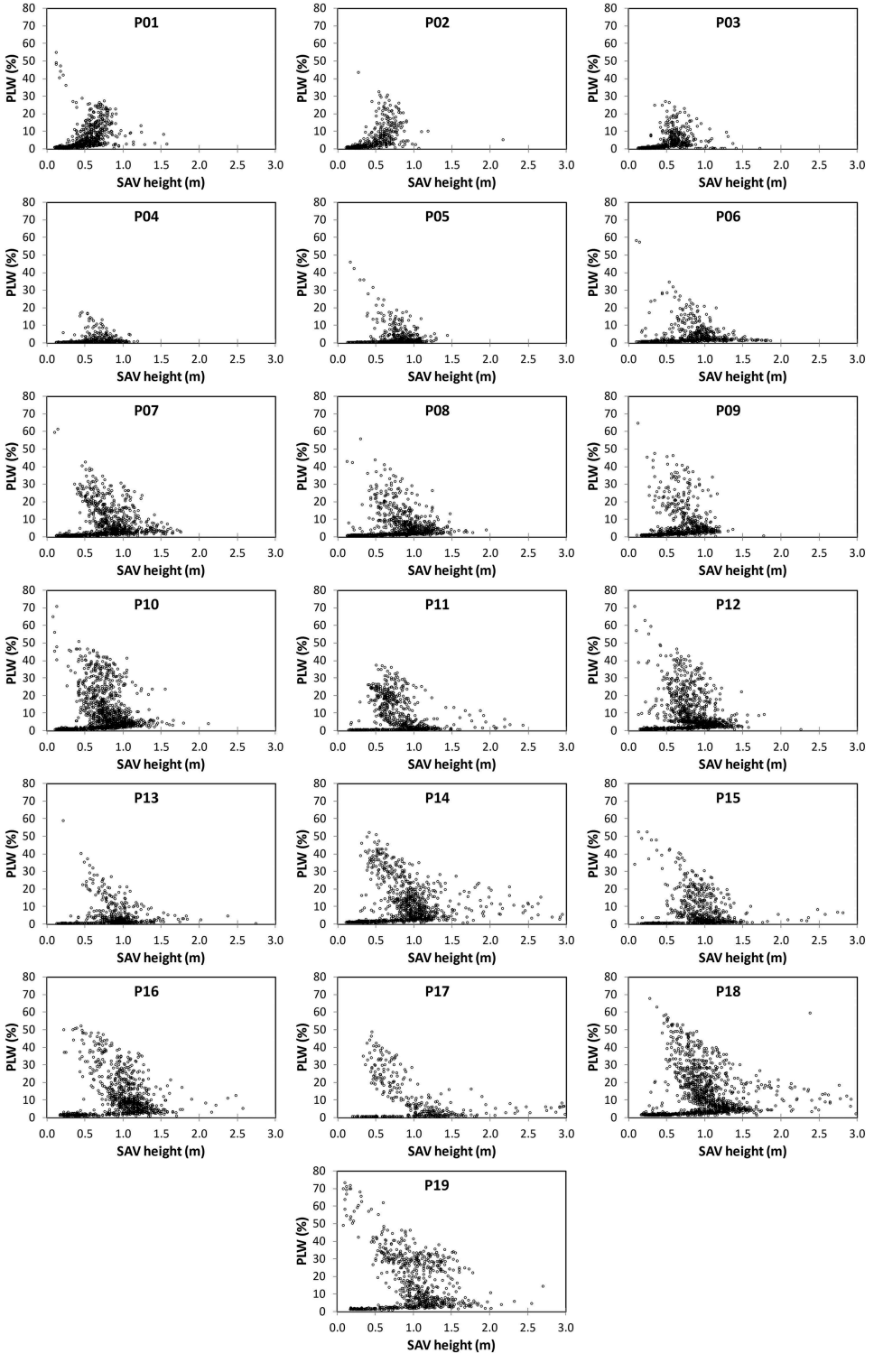

Figure 12. SAV height distribution as a function of PLW at each sampling location.

Bartleson, and Murray (2000, 2004) estimated PLL for Chesapeake Bay SAV in order to compute the minimum light requirement for their growth. The empirical parameterization of PLL proposed by Kemp et al. (2004) was based on DIN and OD. They calculated PLL and PLW to analyse the contributions of water column and epiphytic materials to light attenuation under different water quality conditions in Chesapeake Bay. In tidal freshwater and oligohaline regimes, where Kd < 2 m^{-1} and TSS < 15 mg l^{-1}, the range of PLW and PLL was found to be 0–41 and 0–17%, respectively. However, PLL was not computed in the present study due to the lack of *in situ* data on the primary variables such as epiphytic biomass and DIN. Those data sets will be collected in future field trips in order to estimate PLL and derive the minimum light requirement for SAV growth in Brazilian reservoirs.

SAV height distribution as a function of depth and the euphotic zone limit was analysed. According Figure 13, despite high radiation availability, SAV was not observed in the depth range up to 1 m at any point regions. Upstream regions were marked by high TSS and K_d, and the tallest SAV in that region was 1 m which occurred in relatively shallow waters (around 1 and 2 m deep). In those regions (P01–P06), SAV height decreased as depth increased. Furthermore, in some areas SAV was found beyond the euphotic zone depth but did not occur solely in areas exceeding 8 m in depth. In the downstream (lower K_d) regions from P07 to P19, a slight increase in SAV height was noted as depth increased up to the euphotic zone limit. Beyond the euphotic zone, growth and occurrence were markedly affected. Furthermore, tall SAVs were observed in regions with high Z_{EZ}, such as in P14 to P19. In these regions, maximum SAV height, around 3 m, were recorded (Figure 11(c)). Therefore, the maximum SAV height is highly influenced by K_d. We showed that PLW was directly dependent on depth and K_d, in other words, the greater the depth and K_d, the lower the PLW. The growth of tall SAV was favoured by low PLW, which forces the SAV to grow tall enough to reach the required radiation. In addition, areas with high transparency (lower K_d) can favour the development of high SAV compared to areas with high K_d. This may mean that low PLW values favour SAV height if K_d is low enough not to hinder growth. Finally, maximum and average SAV height decreased from downstream to upstream in the river. Tall SAV occurring in such deep areas may indicate that the studied vegetation has a marked capacity to expand upward in the deeper areas to access the light conditions required for photosynthesis. In summary, the height of the SAV is dependent on two radiative forcings, PLW and K_d (or $K_{d,PAR}$), rather than just K_d as reported by numerous studies previously. This is a finding which has not been previously reported in any freshwater systems.

4. Conclusion

OACs such as TSS and chl-*a* play an important role in SAV distribution and development. Combined with these OACs, K_d and PLW are important optical parameters controlling the attenuation of light in the water column, and can be effectively linked to SAV growth and occurrence. In sampling locations where K_d values were lower, an inverse relationship was observed between SAV height and PLW. With high PLW, the SAV do not have to grow upward to receive sufficient light. On the other hand, in some instances, when PLW decreased the SAV grew taller to receive light required for its development. In such

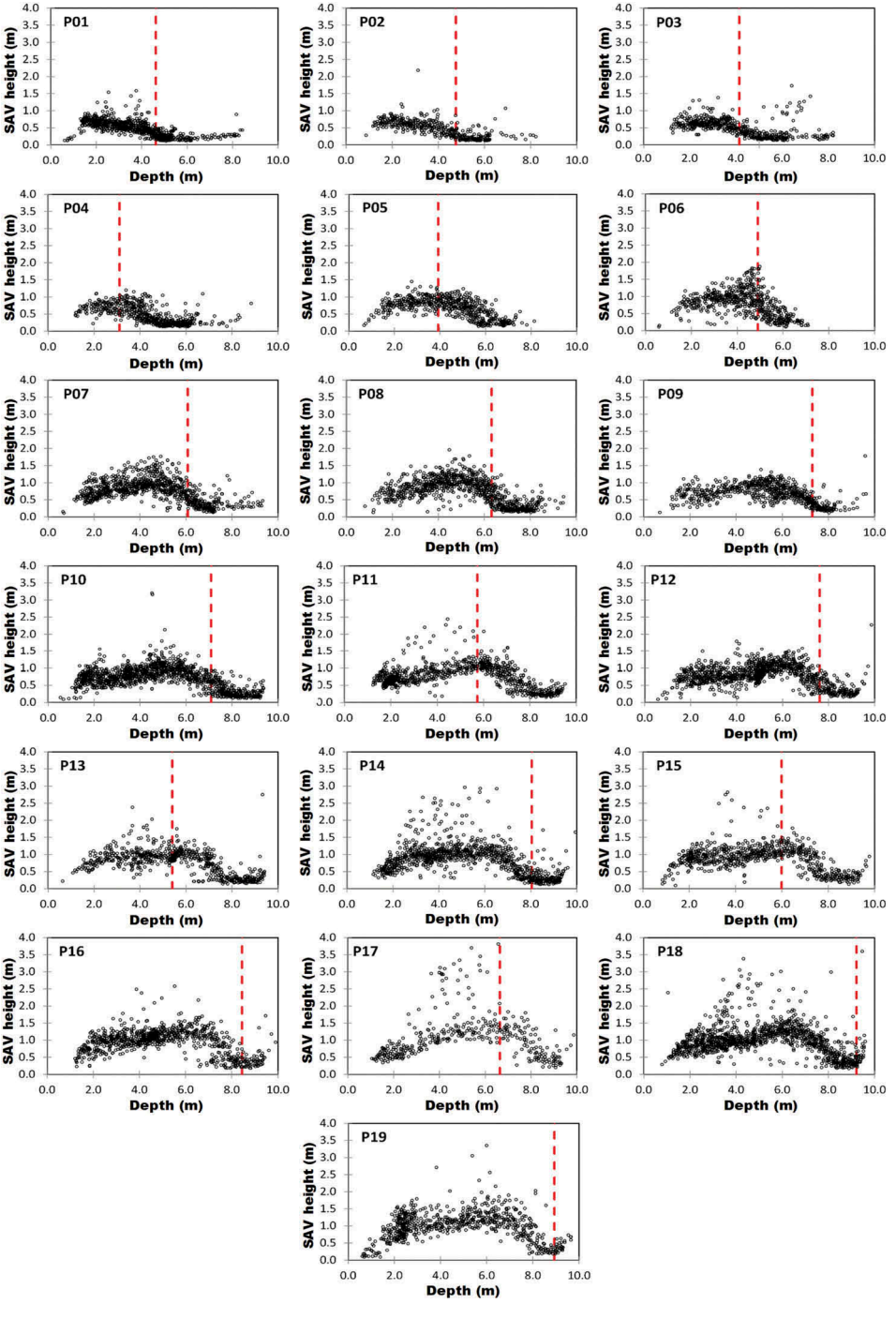

Figure 13. SAV height distribution as a function of depth. The dashed red line represents the euphotic zone limit (Z_{EZ}).

a case, the SAV develops a long, narrow stem resulting in disproportionately lower biomass compared to its height. Low PLW values will favour the development of tall SAV only when K_d is low enough not to interfere with growth. In contrast, points with high transparency (lower K_d) favour the development of tall SAV compared to points with high K_d.

In shallow areas close to the shoreline and up to 1 m deep, the occurrence of SAV is compromised due to either excessive radiation when transparency is high or excessive attenuation when turbidity is high. Rodrigues and Thomaz (2010) and Tavechio and Thomaz (2003) showed that *E. densa* and *E. najas* require low radiation while excessive light levels hinder their development. In addition, waves and variation in water level due to runoff are common in these areas, increasing the likelihood of turbidity impairing SAV growth as shown by Thomaz (2006). A strong inverse relationship between SAV height (average and maximum) and $K_{d,PAR}$ was observed, with correlation coefficient (r) greater than 70% and R^2 greater than 50%. This indicated that SAV height can be estimated by $K_{d,PAR}$ in the study area with significant accuracy. Despite an exponential decrease at greater depths, radiation remained sufficient for regional species' growth because these require only low radiation levels. Therefore, tall SAV was observed in such deep areas because of their marked capacity to expand upward to intercept sufficient light required for photosynthesis. Similar phenomena were observed by Rodrigues and Thomaz (2010), who concluded that greater SAV height is typically observed at greater depths, most likely due to the macrophyte species trait wherein it expands to find sufficient radiation for development.

In general, the SAV grew better in regions with greater transparency and lower K_d. In regions where water depth was greater than the euphotic zone, the presence of SAV should not have occurred because of the lack of radiation for photosynthesis. However, despite a significant decrease in growth, SAV was still found in those areas. We propose two hypotheses to explain these phenomena. First, the aquatic environment can be very dynamic and therefore, the water quality including transparency before, during, and after the field measurements varied considerably, thus creating significant spatial variability in the euphotic zone. Thereby, the SAV found beyond the euphotic zone during our field measurements could have been within the euphotic zone at other times. Second, despite being within the euphotic zone, SAV could have extended, both horizontally and vertically, to intercept PAR for its survival. This behaviour of elongation in *Egeria* is described by Tavechio and Thomaz (2003) and Rodrigues and Thomaz (2010).

Studies on sub-aquatic radiation availability as measured by the vertical attenuation of E_d and $E_{d,PAR}$ in the water column can help in understanding SAV behaviour in tropical reservoirs and therefore contribute to its management. In addition, knowing the concentrations of OACs can provide additional information on the distribution and development of SAV. Beside radiation availability, other limiting factors, not studied here, may influence such behaviour including nutrients, stream velocity, and bottom declivity. Future studies should evaluate SAV growth using variables related to sub-aquatic radiation and other important limiting factors. Finally, we proved that there is a high correlation between SAV and K_d. Therefore, it is strongly recommended that future research studies on estimation of SAV height in tropical reservoirs and even coastal estuaries should use models based on K_d. The methodology developed in this work can be applied to other reservoirs to study spatiotemporal variability in SAV height so that

control measures can be developed to restrict their growth and eliminate various SAV-related problems in reservoirs.

Acknowledgements

The authors thank FAPESP, CNPq, and PPGCC/UNESP for financial support (FAPESP Process No 2012/19821-1 and 2013/09045-7; CNPq Process No 400881/2013-6 and 472131/2012-5; and CNPq for scholarship). Thanks to the University of Georgia for facilitating collaboration between UNESP and UGA through the international student exchange program. A special thanks to Fernanda Watanabe, Thanan Rodrigues, Ulisses Guimarães, Renato Ferreira, and Claudio Barbosa for assisting in field data collection.

Disclosure statement

No potential conflict of interest was reported by the authors.

Funding

This work was supported by FAPESP, CNPq and PPGCC/UNESP (FAPESP Process No 2012/19821-1 and 2013/09045-7; CNPq Process No 400881/2013-6 and 472131/2012-5; and CNPq for scholarship).

ORCID

Deepak R. Mishra http://orcid.org/0000-0001-8192-7681
Enner H. Alcântara http://orcid.org/0000-0002-7777-2119

References

AES Tietê. Accessed 8 may 2013. http://www.aestiete.com.br/

Araújo-Lima, C. A. R. M., A. A. Agostinho, and N. N. Fabré. 1995. "Trophic Aspects of Fish Communities in Brazilian Rivers and Reservoirs." In *Limnology in Brazil*, edited by J. G. Tundisi, C. E. M. Bicudo, and T. Matsumura-Tundisi, 105–136. Rio de Janeiro: ABC/SBL.

Bini, L. M., L. G. Oliveira, D. C. Souza, P. Carvalho, and M. P. Pinto. 2005. "Patterns of The Aquatic Macrophyte Cover in Cachoeira Dourada Reservoir (GO-MG)." *Brazilian Journal of Biology* 65 (1): 19–24. doi:10.1590/S1519-69842005000100004.

Bini, L. M., and S. M. Thomaz. 2005. "Prediction of *Egeria Najas* and *Egeria Densa* Occurrence in a Large Subtropical Reservoir (Itaipu Reservoir, Brazil-Paraguay)." *Aquatic Botany* 83: 227–238. doi:10.1016/j.aquabot.2005.06.010.

Biosonics. 2004a. *User Guide: Visual Acquisition 5.0*. Seattle: Biosonics.

Biosonics. 2004b. "Calibration of BioSonics Digital Scientific Echosounder Using T/C Calibration Spheres." Seattle: Biosonics Inc. Accessed 18 January 2016. http://www.biosonicsinc.com/doc_library/docs/DTXcalibration2e.pdf

Biosonics. 2008. *User Guide: EcoSAV 1*. Seattle: BioSonics.

Biudes, J. F. V., and A. F. M. Camargo. 2008. "Studying the Limitant Factors to Primary Production of Aquatic Macrophytes in Brazil." [Estudos dos Fatores Limitantes à Produção Primária por Macrófitas Aquáticas no Brasil.]*Oecologia Brasiliensis* 12 (1): 7–19. doi:10.4257/oeco.2008.1201.01.

Caffrey, A. J., M. V. Hoyer, and D. E. CanfieldJr. 2007. "Factors Affecting the Maximum Depth of Colonization by Submersed Macrophytes in Florida Lakes." *Lake and Reservoir Management* 23 (3): 287–297. doi:10.1080/07438140709354017.

Camargo, A. F. M., M. M. Pezzato, and G. G. Henry-Silva. 2003. "Limitant Factors to Primary Production of Aquatic Macrophytes." [Fatores limitantes à produção primária macrófitas aquáticas.] In *Ecologia e manejo de macrófitas aquáticas*, edited byS. M. Thomaz and L. M. Bini, 59–83. Mariná: EDUEM.

Carpenter, S. R., and D. M. Lodge. 1986. "Effects of Submersed Macrophytes on Ecosystem Processes." *Aquatic Botany* 26: 341–370. doi:10.1016/0304-3770(86)90031-8.

Cavenaghi, A. L., E. D. Velini, M. L. T. B. Galo, F. T. Carvalho, E. Negrisoli, M. L. B. Trindade, and J. L. A. Simionato. 2003. "Characterization of Water Quality and Sediment Related to the Occurrence of Aquatic Plants in Five Tietê Waterhed Reservoirs." [Caracterização da Qualidade de Água e Sedimento Relacionados com a Ocorrência de Plantas Aquáticas em Cinco Reservatórios da Bacia do Rio Tietê.] *Planta Daninha* 21: 43–52. doi:10.1590/S0100-83582003000400007.

CBH-BT/CETEC. 1999. "Hydrographic Basin Committee of Baixo Tietê." [Comitê da Bacia Hidrográfica do Baixo Tietê.]Centro Tecnológico da Fundação Paulista de Tecnologia e Educação. Situação dos Recursos Hídricos do Baixo Tietê – Minuta preliminar do relatório técnico final. Lins: CBH-BT. Accessed 8 May 2013. http://www.sigrh.sp.gov.br/sigrh/ARQS/RELATORIO/CRH/CBH-BT/232/relbtseg.pdf

Chamberlain, R. H., P. H. Doening, B. Orlando, and B. M. Sabol. 2009. "Comparison of Manual and Hydroacoustic Measurement of Seagrass Distribution in the Caloosahatchee Estuary, Florida." *Florida Scientist* 72: 386–405.

Cho, H. J. 2007. "Effects of Prevailing Winds on Turbidity of a Shallow Estuary." *International Journal of Environmental Research and Public Health* 4 (2): 185–192. doi:10.3390/ijerph2007040014.

Clesceri, L. S., A. E. Greenberg, and A. D. Eaton. 1998. *Standard Methods for the Examination of Water and Wastewater*. Washington: American Public Health Association.

Esteves, F. A. 2011. *Fundamentos de Limnologia*. 3rd ed. Rio de Janeiro: Interciência.

Gallegos, C. L. 2001. "Calculating Optical Water Quality Targets to Restore and Protect Submersed Aquatic Vegetation: Overcoming Problems in Partitioning the Diffuse Attenuation Coefficient for Photosynthetically Active Radiation." *Estuaries* 24 (3): 381–397. doi:10.2307/1353240.

Golterman, H. L., R. S. Clymo, and M. A. M. Ohnstad. 1978. *Methods for Physical and Chemical Analysis of Fresh Waters*. 2nd ed. Oxford: Blackwell Scientific.

Havens, K. E. 2003. "Submerged Aquatic Vegetation Correlations with Depth and Light Attenuating Materials in a Shallow Subtropical Lake." *Hydrobiologia* 493: 173–186. doi:10.1023/A:1025497621547.

Isaaks, E. H., and R. Srivastava. 1989. *An Introduction to Applied Geostatistics*. New York: Oxford University Press.

Jakubauskas, M. E., D. L. Peterson, S. W. Campbell, F. de Noyelles Jr., S. D. Campbell, and D. Penny. 2002. "Mapping and Monitoring Invasive Aquatic Plant Obstructions in Navigable Waterways Using Satellite Multispectral Imagery." In *Pecora 15/Land Satellite Information IV/ISPRS Commission I/FIEOS* 2002 *Conference Proceedings*, edited by S. Morain and A. Budge, Denver, CO.

Kemp, W. M., R. Bartleson, and L. Murray. 2000. "Epiphyte Contributions to Light Attenuation at the Leaf Surface." Chap. 5in *Chesapeake Bay Submerged Aquatic Vegetation Water Quality and Habitat-Based Requirements and Restoration Targets*, edited by R. Batiuk, R. Orth, K. Moore, J. C. Stevenson, W. Dennison, L. Staver, V. Carter, et al., 55–70. A Second Technical Synthesis. Chesapeake Bay Program, Annapolis, MD: CBP/TRS 245/00.EPA 903-R-00-014.U.S.EPA.

Kemp, W. M., R. Batiuk, R. Bartleson, P. Bergstrom, V. Carter, C. L. Gallegos, W. Hunley, et al. 2004. "Habitat Requirements for Submerged Aquatic Vegetation in Chesapeake Bay: Water Quality, Light Regime, and Physical-Chemical Factors." *Estuaries* 27 (3): 363–377. doi:10.1007/BF02803529.

Kirk, J. T. O. 2011. *Light and Photosynthesis in Aquatic Ecosystems*. 3rd ed. New York: Cambridge University Press.

Marcondes, D. A. S., A. L. Mustafá, and R. H. Tanaka. 2003. "Estudos para Manejo Integrado de Plantas Aquáticas no Reservatório de Jupiá." Chap 15 in*Ecologia e Manejo de Macrófitas*

Aquáticas, edited byS. M. Thomaz and L. M. Bini, 299–317. Maringá: EDUEM. http://www.eduem.uem.br/livros/ebook/ebook_eemdma.pdf

Mishra, D. R., S. Narumalani, D. Rundquist, and M. Lawson. 2005. "Characterizing the Vertical Diffuse Attenuation Coefficient for Downwelling Irradiance in Coastal Waters: Implications for Water Penetration by High Resolution Satellite Data." *ISPRS Journal of Photogrammetry and Remote Sensing* 60: 48–64. doi:10.1016/j.isprsjprs.2005.09.003.

Mishra, D. R., S. Narumalani, D. Rundquist, M. Lawson, and R. Perk. 2007. "Enhancing The Detection and Classification of Coral Reef and Associated Benthic Habitats: A Hyperspectral Remote Sensing Approach." *Journal of Geophysical Research: Oceans* 112 (C8): 1–18. doi:10.1029/2006JC003892.

Mishra, D. R., S. Narumalani, D. Rundquist, and M. P. Lawson. 2006. "Benthic Habitat Mapping in Tropical Marine Environments using QuickBird Imagery." *Photogrammetric Engineering and Remote Sensing* 72 (9): 1037–1048. doi:10.14358/PERS.72.9.1037.

Mishra, S., D. R. Mishra, and Z. Lee. 2014. "Bio-optical Inversion in Highly Turbid and Cyanobacteria Dominated Waters." *IEEE Transactions in Geosciences and Remote Sensing* 52 (1): 375–388. doi:10.1109/TGRS.2013.2240462.

Mishra, S., D. R. Mishra, Z. Lee, and C. Tucker. 2013. "Quantifying Cyanobacterial Phycocyanin Concentration in Turbid Productive Waters: A Quasi-analytical Approach." *Remote Sensing of Environment* 133: 141–151. doi:10.1016/j.rse.2013.02.004.

Mobley, C. D. 1994. *Light and Water: Radiative Transfer in Natural Waters*. San Diego: Academic Press.

Mueller, J. L. 2003. "In-Water Radiometric Profile Measurements and Data Analysis Protocols." Chap 2 in *Ocean Optics Protocols for Satellite Ocean Color Sensor Validation Revision 4, Volume III*, edited byJ. L. Mueller, G. S. Fargion, and C. R. McClain. Maryland: NASA, Goddard Space Flight Space Center. http://oceancolor.gsfc.nasa.gov/DOCS/Protocols_Ver4_VolIII.pdf

Rockwell, H. W. 2003. "Summary of a Survey of the Literature on the Economic Impact of Aquatic Weeds." In *The economic impact of aquatic weeds*. Report for the Aquatic Ecosystem Restoration Foundation. Accessed12August2015. http://www.aquatics.org/pubs/economics.html

Rodgher, S., E. L. G. Espíndola, O. Rocha, R. Fracácio, R. H. G. Pereira, and M. H. S. Rodrigues. 2005. "Limnological and Ecotoxicological Studies in the Cascade of Reservoirs in the Tietê River (São Paulo, Brazil)." *Brazilian Journal of Biology* 65 (4): 697–710. doi:10.1590/S1519-69842005000400017.

Rodrigues, R. B., and S. M. Thomaz. 2010. "Photosynthetic and Growth Responses of *Egeria Densa* to Photosynthetic Active Radiation." *Aquatic Botany* 92 (4): 281–284. doi:10.1016/j.aquabot.2010.01.009.

Rotta, L. H. S., N. N. Imai, L. F. A. Batista, L. S. Boschi, M. L. B. T. Galo, and E. D. Velini. 2012. "Hydro-Acoustic Remote Sensing in Submerged Aquatic Macrophyte Mapping." *Planta Daninha* 30 (2): 229–239. doi:10.1590/S0100-83582012000200001.

Sabol, B. M., R. E. MeltonJr., R. Chamberlain, P. Doering, and K. Haunert. 2002. "Evaluation of A Digital Echo Sounder System for Detection of Submersed Aquatic Vegetation." *Estuaries* 25 (1): 133–141. doi:10.1007/BF02696057.

Schwarz, A. M., M. Wintonb, and I. Hawes. 2002. "Species-Specific Depth Zonation in New Zealand Charophytes as a Function of Light Availability." *Aquatic Botany* 72 (3–4): 209–217. doi:10.1016/S0304-3770(01)00201-7.

SSRH/CRHi. 2011. Secretaria de Saneamento e Recursos Hídricos, Coordenadoria de Recursos Hídricos: Situação dos Recursos Hídricos no Estado de São Paulo, Ano base 2009. Accessed8May2013. http://www.sigrh.sp.gov.br/sigrh/basecon/RelatorioSituacao2011/Relatorio_Situacao_2011.pdf

Tavechio, W. L. G., and S. M. Thomaz. 2003. "Effects of Light on the Growth and Photosynthesis of *Egeria najas* Planchon." *Brazilian Archives of Biology and Technology* 46 (2): 203–209. doi:10.1590/S1516-89132003000200011.

Thomaz, S. M. 2006. "Fatores que Afetam a Distribuição e o Desenvolvimento de Macrófitas Aquáticas em Reservatórios: Uma Análise em Diferentes Escalas." In *Ecologia de Reservatórios:*

Impactos Potenciais, Ações de Manejo e Sistemas em Cascata, edited by M. G. Nogueira, R. Henry, and A. Jorcin. São Carlos: RiMa.

Thomaz, S. M., and L. M. Bini. 1998. "Ecologia e Manejo de Macrófitas Aquáticas em Reservatórios." *Acta Limnologica Brasiliensia* 10 (1): 103–116.

Thomaz, S. M., F. A. Esteves, K. J. Murphy, A. M. Dos-Santas, A. Caliman, and R. D. Guariento. 2008. "Aquatic Macrophytes in the Tropics: Ecology of Population and Communities, Impact of Invasion and Use by Man." *Tropical Biology and Conservation Management* 4: 33–37.

Tundisi, J. G., and T. M. Tundisi. 2008. *Limnologia*. São Paulo: Oficina de Textos.

Twilley, R. R., W. M. Kemp, K. W. Staver, J. C. Stevenson, and W. R. Boynton. 1985. "Nutrient Enrichment of Estuarine Submersed Vascular Plant Communities. 1. Algal Growth and Effects on Production of Plants and Associated Communities." *Marine Ecology* 23 (2): 179–191. doi:10.3354/meps023179.

Wetzel, R. G. 2001. *Limnology: Lake and River Ecosystems*. 3rd ed. San Diego: Academic press.